NeuroImage 288 (2024) 120534

Contents lists available at ScienceDirect

NeuroImage

journal homepage: www.elsevier.com/locate/ynimg

Whole-brain structural connectome asymmetry in autism

Seulki Yoo [a], Yurim Jang [b], Seok-Jun Hong [c,d], Hyunjin Park [d,e], Sofie L. Valk [f,g,h], Boris C. Bernhardt [i], Bo-yong Park [d,j,k,*]

[a] Convergence Research Institute, Sungkyunkwan University, Suwon, Republic of Korea
[b] Artificial Intelligence Convergence Research Center, Inha University, Incheon, Republic of Korea
[c] Department of Biomedical Engineering, Sungkyunkwan University, Suwon, Republic of Korea
[d] Center for Neuroscience Imaging Research, Institute for Basic Science, Suwon, Republic of Korea
[e] School of Electronic and Electrical Engineering, Sungkyunkwan University, Suwon, Republic of Korea
[f] Forschungszentrum Julich, Germany
[g] Max Planck Institute for Cognitive and Brain Sciences, Leipzig, Germany
[h] Systems Neuroscience, Heinrich Heine University, Duesseldorf, Germany
[i] McConnell Brain Imaging Centre, Montreal Neurological Institute and Hospital, McGill University, Montreal, Quebec, Canada
[j] Department of Data Science, Inha University, Incheon, Republic of Korea
[k] Department of Statistics and Data Science, Inha University, Incheon, Republic of Korea

ARTICLE INFO

Keywords:
Autism
Structural connectivity
Brain asymmetry
Network communication
Machine learning

ABSTRACT

Autism spectrum disorder is a common neurodevelopmental condition that manifests as a disruption in sensory and social skills. Although it has been shown that the brain morphology of individuals with autism is asymmetric, how this differentially affects the structural connectome organization of each hemisphere remains under-investigated. We studied whole-brain structural connectivity-based brain asymmetry in individuals with autism using diffusion magnetic resonance imaging obtained from the Autism Brain Imaging Data Exchange initiative. By leveraging dimensionality reduction techniques, we constructed low-dimensional representations of structural connectivity and calculated their asymmetry index. Comparing the asymmetry index between individuals with autism and neurotypical controls, we found atypical structural connectome asymmetry in the sensory and default-mode regions, particularly showing weaker asymmetry towards the right hemisphere in autism. Network communication provided topological underpinnings by demonstrating that the inferior temporal cortex and limbic and frontoparietal regions showed reduced global network communication efficiency and decreased send-receive network navigation in the inferior temporal and lateral visual cortices in individuals with autism. Finally, supervised machine learning revealed that structural connectome asymmetry could be used as a measure for predicting communication-related autistic symptoms and nonverbal intelligence. Our findings provide insights into macroscale structural connectome alterations in autism and their topological underpinnings.

1. Introduction

Autism spectrum disorder is a highly heritable and heterogeneous neurodevelopmental condition characterized by impaired social communication, restricted and repetitive behavior, and atypical sensory processing (Baio et al., 2018; Christensen et al., 2018; Mottron et al., 2006). These symptoms are associated with brain network disorganization and altered neuronal processing, particularly excitation/inhibition imbalances (Jou et al., 2011; Lee et al., 2017; Nelson and Valakh, 2015; Nunes et al., 2019; Sohal and Rubenstein, 2019). Previous studies have investigated the multiscale properties of the autistic brain by studying network-level brain connectomics and local microcircuit function to better understand the pathological and behavioral phenotypes of autism (Hong et al., 2019; Lee et al., 2017; Nair et al., 2013; Nelson and Valakh, 2015; Nunes et al., 2019; Park et al., 2021c).

Early studies based on magnetic resonance imaging (MRI) observed morphological and connectivity changes in the brains of individuals with autism. For example, they found increases in regional gray matter volume and cortical thickness (Khundrakpam et al., 2017; Valk et al., 2015; Zhou et al., 2014), as well as cortico-cortical functional

* Corresponding author at: Department of Data Science, Inha University, Incheon, the Republic of Korea.
E-mail address: boyong.park@inha.ac.kr (B.-y. Park).

https://doi.org/10.1016/j.neuroimage.2024.120534
Received 8 September 2023; Received in revised form 28 January 2024; Accepted 7 February 2024
Available online 8 February 2024

hypoconnectivity and cortico-subcortical hyperconnectivity (Cerliani et al., 2015; Di Martino et al., 2014). Recent studies have reported abnormal brain morphology and structural network organization at the regional and large-scale network levels using a large dataset obtained from the Enhancing NeuroImaging Genetics through Meta-Analysis (ENIGMA) consortium (Postema et al., 2019; Sha et al., 2022; Van Rooij et al., 2018).

The whole-brain connectome organization can be plotted using an advanced model based on manifold learning (*i.e.*, dimensionality reduction techniques) (Haak et al., 2018; Huntenburg et al., 2018; Margulies et al., 2016). This approach offers a compact perspective on the large-scale connectome organization of the brain by estimating low-dimensional representations of connectivity (*i.e.*, eigenvectors), which may reflect the heterogeneity and multiplicity of a brain region (Haak and Beckmann, 2020; Haak et al., 2018; Margulies et al., 2016). Previous studies used these techniques to investigate biologically meaningful cortical axes. The first principal component of functional connectivity represents the hierarchical sensory-fugal axis along the cortex (Margulies et al., 2016), and that derived from the microstructural (Paquola et al., 2019) and structural connectivity (Park et al., 2021d) showed comparable cortical axes. In particular, studies on autism datasets have used these techniques to assess altered brain structure and function. Functional connectome organization showed atypicality in low-level sensory and higher-order default-mode regions in individuals with autism compared to neurotypical controls (Hong et al., 2019). Diffusion MRI tractography quantifies spatial patterns of neuronal streamlines connecting different brain regions by delineating pathways connecting different brain regions through the axonal fiber bundles in the white matter. Our previous study investigated structural connectome organization using the manifold learning approach and observed structural connectome alterations in sensory, somatomotor, and heteromodal association cortices (Park et al., 2021a, 2021c). Likewise, individuals with autism show atypical structural and functional brain organization, and the manifold learning approach might be a useful technique for investigating autistic brains.

The inter-hemispheric asymmetry of brain structures, such as surface area and cortical thickness, has been recently investigated and provided information for understanding the lateralization of the brain (Khundrakpam et al., 2017; Kong et al., 2018; Postema et al., 2019; Sha et al., 2022). For example, atypical brain asymmetry patterns were found in various neuropsychiatric conditions such as schizophrenia, attention-deficit/hyperactivity disorder, and autism spectrum disorder (Okada et al., 2016; Postema et al., 2021, 2019; Sha et al., 2022). Previous studies have shown that atypical asymmetry of brain structure is associated with altered cognitive function in language, motor, attention, and memory systems, which may lead to neurological and psychiatric conditions (Balathay et al., 2023; Pinto et al., 2023; Wang et al., 2023).

In individuals with autism, the ENIGMA study observed reduced cortical thickness asymmetry in frontal, cingulate, and temporal cortices (Postema et al., 2019). These asymmetry patterns were associated with the symptom severity of autism and showed differential developmental trajectory compared to the neurotypical controls, particularly in language-related abilities (Dougherty et al., 2016; Herbert et al., 2002). These explorations imply that various forms of lateralization in brain structure and function characterize autism. However, the underlying topology or communication mechanism regarding the atypical brain asymmetry in autism is still unknown. Although there is a controversy about whether the abnormal asymmetry in brain structure or function in individuals with autism stems from a shift in connectivity towards a specific hemisphere or from a reduction in hemispheric specialization in connectivity (Floris et al., 2021), it is obvious that the atypical asymmetry of brain structure is associated with altered cognitive function, which may lead to disease occurrence and symptom progression. In this study, to fill the gap in understanding brain asymmetry in autism, we aimed to quantitatively investigate whole-brain structural connectome asymmetry in individuals with autism by employing the manifold learning approach.

Network communication models may reveal the underlying topography of structural connectome asymmetry by indirectly inferring the directionality of large-scale neural signaling (Avena-Koenigsberger et al., 2018, 2019; Goñi et al., 2014; Seguin et al., 2018). These models measure the efficiency of information flow between different brain regions. For example, the network can be depicted with a spectrum of communication processes based on the shortest path communication (*i.e.,* routing) at one extreme and random walk processes (*i.e.,* diffusion) at the other extreme (Avena-Koenigsberger et al., 2018, 2019). Prior works widely adopted these network communication models to investigate the brain topology of cortical hierarchies (Vázquez-Rodríguez et al., 2019; Vézquez-Rodríguez et al., 2020) and functional dynamics (Avena-Koenigsberger et al., 2018; Park et al., 2021b, 2021d; Seguin et al., 2022). Thus, we hypothesized that these network communication models provide insights into the topological underpinnings of structural connectome asymmetry in autism.

Expanding upon prior studies that explored inter-hemispheric asymmetry of brain morphology (Khundrakpam et al., 2017; Kong et al., 2018; Postema et al., 2019; Sha et al., 2022), we investigated perturbations in structural connectome asymmetry in individuals with autism. We first estimated low-dimensional representations of structural connectivity based on dimensionality reduction techniques (Coifman and Lafon, 2006; Margulies et al., 2016) and assessed between-group differences in connectome asymmetry between individuals with autism and neurotypical controls. We then compared network communication measures between the groups to assess whether individuals with autism showed altered network communication. Finally, we utilized supervised machine learning to predict behavioral assessments calibrated by the Autism Diagnostic Observation Schedule (ADOS—social cognition, communication, and repetitive behavior/interest sub-scores and total score) and intelligence quotient (IQ).

2. Methods

2.1. Study participants

We analyzed T1-weighted MRI and diffusion MRI data of 80 individuals with autism (mean ± SD age= 12.1 ± 4.9 years; 15% female) and 61 healthy controls (mean ± SD age= 13.2 ± 4.0 years; 4.9% female) obtained from Autism Brain Imaging Data Exchange initiative (ABIDE-II; https://fcon_1000.projects.nitrc.org/indi/abide) (Di Martino et al., 2017, 2014) (**Supplementary Table 1**). Among multiple sites, we included the sites that (i) contained children and adults with autism and neurotypical controls, with ≥10 individuals per group, (ii) who had T1-weighted and diffusion MRI available, and (iii) sufficient MRI data quality (*i.e.,* scanned with 3T scanner and appropriate b-value and b-vector files). Finally, three sites from the ABIDE database were included: New York University Langone Medical Center (NYU), Trinity College Dublin (TCD), and San Diego State University (SDSU). According to gold standard diagnostic methods, all individuals with autism were diagnosed using the ADOS (Lord et al., 2000) and/or the Autism Diagnostic Interview-Revised (Lord et al., 1994). Only the NYU and TCD sites provided IQ scores, and they were measured using the Wechsler Abbreviated Scale of Intelligence (WASI) series or Differential Ability Scales (DAS). Out of 84 subjects from these sites, 72 used WASI, and others used DAS. ABIDE data collection was performed in accordance with the local Institutional Review Board (IRB) guidelines. All sites confirmed that their local ethics committee has approved the initial data collection and the retrospective sharing of a fully de-identified version of the datasets (Di Martino et al., 2017). Following the Health Insurance Portable and Accountability Act (HIPAA) guidelines and the 1000 Functional Connectomes Project/INDI protocols, all ABIDE datasets were fully anonymized, with no protected health information identifiers included.

2.2. Data acquisition

Multimodal MRI data from T1-weighted and diffusion MRI were acquired at three independent sites. At the NYU site, all data was acquired using a 3T Siemens Allegra scanner. The T1-weighted images were obtained using a 3D magnetization prepared rapid acquisition gradient echo (MPRAGE) sequence (repetition time (TR)= 2530 ms; echo time (TE)= 3.25 ms; inversion time (TI)= 1100 ms; flip angle (FA)= 7°; matrix size= 256 × 192; and voxel size= 1.3 × 1.0 × 1.3 mm^3). Diffusion MRI data were obtained using a 2D spin echo-echo planar imaging (SE-EPI) sequence (TR= 5200 ms; TE= 78 ms; matrix size= 64 × 64; voxel size= 3 mm^3, isotropic; 64 directions; b-value= 1000 s/mm^2; and 1 b0 image). At the TCD site, the participants were scanned using a 3T Philips Achieva. The T1-weighted data were acquired using a 3D MPRAGE sequence (TR= 8400 ms; TE= 3.90 ms; TI= 1150 ms; FA= 8°; matrix= 256 × 256; voxel size= 0.9 mm^3, isotropic) and diffusion MRI data using a 2D SE-EPI (TR= 20,244 ms; TE= 7.9 ms; matrix size= 124 × 124; voxel size= 1.94 × 1.94 × 2 mm^3; 61 directions; b-value= 1500s/mm^2; and 1 b0 image). At the SDSU site, all data was acquired using a 3T GE MR7550 scanner. The T1-weighted images were acquired using a 3D standard fast spoiled gradient echo (SPGR) sequence (TR= 8.136 ms; TE= 3.172 ms; TI= 600 ms; FA= 8°; matrix size= 256 × 192; and voxel size= 1mm^3 isotropic) and diffusion MRI were scanned using a 2D SE-EPI sequence (TR= 8500 ms; TE= 84.9 ms; matrix size= 128 × 128; voxel size= 1.875 × 1.875 × 2 mm^3; 61 directions; b-value= 1000 s/mm^2; and 1 b0 image).

2.3. Data preprocessing

a) *T1-weighted MRI:* The T1-weighted data were preprocessed using FreeSurfer. First, variations in image intensities caused by magnetic field nonuniformities were corrected, and non-brain tissue was removed. The intensity normalization was performed to correct variations in intensity values, and tissue segmentation was conducted to classify the voxels into different tissue types, including gray matter, white matter, and cerebrospinal fluid. Surface reconstruction was performed using topology correction, inflation, and spherical registration to the fsaverage template space (Dale et al., 1999; Fischl et al., 2001, 1999a, 1999b; Ségonne et al., 2007).

b) *Diffusion MRI:* The diffusion MRI data were processed using MRtrix3 (Tournier et al., 2019). The distortions induced by eddy currents and B0 field inhomogeneity were corrected to mitigate geometric distortions, especially in areas close to the air-filled sinuses and air cells in the skull. Then, the head motion was corrected to obtain a consistent orientation and location across the volumes. Structural connectomes were generated from preprocessed diffusion MRI using MRtrix3 (Tournier et al., 2019).

2.4. Structural connectome generation

We constructed the structural connectivity matrix using MRtrix3 (Tournier et al., 2019). Anatomically constrained tractography was performed based on different tissue types defined using T1-weighted images (Smith et al., 2012). Multi-shell and multi-tissue response functions were estimated (Christiaens et al., 2015), and constrained spherical deconvolution and intensity normalization were performed (Jeurissen et al., 2014). The tractogram was generated based on a probabilistic approach (Tournier et al., 2019, 2010, 2012) with 40 million streamlines, a maximum tract length of 250, and a fractional anisotropy cutoff of 0.06. Subsequently, spherical deconvolution informed filtering of tractograms (SIFT2) was applied to optimize the cross-section multiplier for each streamline (Smith et al., 2015). We constructed a structural connectome by mapping the reconstructed cross-section streamlines onto the Schaefer atlas with 200 parcels (Schaefer et al., 2018) and log-transformed the values to adjust for the scale (Fornito et al., 2016).

2.5. Low-dimensional representations of structural connectivity

We estimated cortex-wide low-dimensional representations of structural connectivity (*i.e.,* eigenvectors) using nonlinear dimensionality reduction techniques implemented in BrainSpace (https://github.com/MICA-MNI/BrainSpace) (Vos de Wael et al., 2020). Specifically, we generated a group-representative structural connectivity matrix based on distance-dependent thresholding that preserves long-range connections (Betzel et al., 2019) and estimated the eigenvectors via diffusion map embedding (Coifman and Lafon, 2006). The diffusion map embedding algorithm is robust to noise and is computationally efficient compared to other nonlinear manifold learning techniques (Tenenbaum et al., 2000; Von Luxburg, 2007). It is controlled by two parameters, α and t, where α controls the influence of the density of sampling points on the manifold (α= 0, maximal influence; α= 1, no influence) and t controls the scale of the eigenvalues of the diffusion operator. We set α= 0.5 and t = 0 to retain the global relations between data points in the embedded space, following prior applications (Hong et al., 2019; Margulies et al., 2016; Paquola et al., 2019; Park et al., 2021c; Vos de Wael et al., 2020). After generating the template eigenvectors, individual eigenvectors were estimated and aligned to the template via Procrustes alignment (Langs et al., 2015; Vos de Wael et al., 2020).

2.6. Structural connectome asymmetry and between-group differences

We adopted the Schaefer atlas and matched the parcels of the left and right hemispheres based on their overlap ratios, as it is an asymmetric parcellation scheme (Schaefer et al., 2018). We then calculated the asymmetry index of each eigenvector as follows:

$$AI = (L-R) \Big/ \left| \frac{L+R}{2} \right|,$$

where AI is the asymmetry index and L and R indicate the eigenvector values of the left and right hemispheres, respectively (Bernasconi et al., 2003; Kong et al., 2018; Sarica et al., 2018). The positive value indicates that the left hemisphere has higher eigenvector values, while the negative value is *vice versa*. As the eigenvectors generated from the structural connectivity represent connectome organization at a large scale, the asymmetry index reflects the asymmetry of brain structure. We assessed the between-group differences in the asymmetry index between individuals with autism and neurotypical controls using the SurfStat toolbox (https://www.math.mcgill.ca/keith/surfstat/) (Chung et al., 2010; Worsley et al., 2009). We controlled for age, sex, and site from the asymmetry indices calculated from multiple eigenvectors and implemented the multivariate linear models based on Hotelling's T statistics. Specifically, we assessed between-group differences in the asymmetry indices (response variables) between the autism and control groups (explanatory variable) (Chung et al., 2010; Worsley et al., 2009). Multiple comparisons across brain regions were corrected using the false discovery rate (FDR) < 0.05 (Benjamini and Hochberg, 1995). We then stratified the between-group difference effects according to seven intrinsic networks (Yeo et al., 2011) and a cortical hierarchical organization (Mesulam, 1998).

2.7. Subcorico-cortical connectivity

In addition to the atypical asymmetry of cortico-cortical connectivity, we investigated subcortico-cortical connectivity. For each individual, subcortical regions were defined using FSL's FIRST, which generates the accumbens, amygdala, pallidum, caudate, hippocampus, thalamus, and putamen (Patenaude et al., 2011). Subcortical-weighted manifolds were calculated by element-wise multiplication of subcortico-cortical connectivity with cortical eigenvectors (Park et al., 2021a, 2021c), and the nodal degree of the subcortical-weighted manifolds was calculated. We then assessed between-group differences in nodal degree

values between individuals with autism and neurotypical controls after controlling for age, sex, and site. The multiple comparisons across subcortical regions were corrected using FDR < 0.05 (Benjamini and Hochberg, 1995).

2.8. Network communication measures

It has been shown that individuals with autism exhibit atypical brain connectivity patterns in terms of network communications (Guo et al., 2019; Lewis et al., 2014; Zhang et al., 2022), indicating the possible links between the connectome disorganization in individuals with autism and altered network communications. To investigate the connection strengths as well as the network communication efficiency of regions that showed atypical structural connectome asymmetry, we assessed structural connectivity and navigation efficiency between the seed and target regions. Structural connectivity provides information about the strengths of anatomical connections between different brain regions, and navigation efficiency measures how quickly information traverses between two different nodes (Seguin et al., 2018). The seed regions showed significant between-group differences in asymmetry index between individuals with autism and neurotypical controls, and the target regions were seven intrinsic functional communities, including visual, somatomotor, dorsal attention, ventral attention, limbic, frontoparietal, and default-mode networks (Yeo et al., 2011). For each participant, we stratified the structural connectivity and navigation efficiency between the seed and target regions to assess the relationship between communication ability and connection strength. Statistical differences in the features between the groups were assessed using a two-sample *t*-test with 1000 permutation tests. We randomly assigned autism and control groups and constructed a null distribution using t-statistics derived from the null groups. The p-value was calculated by dividing the number of permuted t-statistic values that were larger than the real t-statistic by the number of permutations. Multiple comparisons were corrected using FDR < 0.05 (Benjamini and Hochberg, 1995).

2.9. Send-receive communication of navigation efficiency

To provide topological connectome underpinnings of regions that showed atypical structural connectome asymmetry, we assessed the send-receive communication of navigation efficiency. Navigation efficiency is a measure quantifying information transfer efficiency using a greedy routing algorithm based on the distance between different nodes. Specifically, it measures the efficiency of the progression of a given node to the next directly connected node to reach the target node based on the shortest path mechanism. This measure is asymmetric, where the navigation in the path starting from a given node and that in the path arriving from other nodes to the given node are different. It can be conceptualized using send-receive communication through the observed paths (Seguin et al., 2018). Specifically, the sending navigation efficiency measures how effectively a network transmits signals or information to other brain regions, and the receiving navigation efficiency assesses how effectively a certain brain area utilizes the information received from other regions. We assessed differences in send or receive of navigation efficiency between individuals with autism and neurotypical controls using two-sample *t*-tests with 1000 permutation tests, and the multiple comparisons across the seeds were corrected using FDR < 0.05 (Benjamini and Hochberg, 1995).

2.10. Prediction of behavioral phenotypes

By leveraging supervised machine learning, we predicted behavioral phenotypes of individuals with autism, including ADOS social cognition, communication, repetitive behavior/interest sub-scores, total score, and verbal and performance IQ and their ratio (*i.e.*, verbal/performance IQ) using the asymmetry index of the whole cortex controlled for age, sex, and site. For each phenotype, we first assessed the regression coefficients of each independent variable using ridge regression (McDonald, 2009). The linear combination of the features and ridge coefficients was calculated to obtain the predicted phenotype score and was compared with the actual score. We performed the above process with a five-fold cross-validation, where four of the five partitions were used as training data, and the remaining partition was used as test data. Performance was assessed using Spearman correlations between the actual and predicted phenotype scores, and significance was assessed using 1000 permutation tests. The FDR procedure was applied to correct for multiple comparisons across behavioral phenotypes (Benjamini and Hochberg, 1995). In addition, we calculated the intra-class correlation coefficient (ICC) and mean absolute error. As the ADOS scores were measured using multiple modules at the NYU site, we additionally performed the prediction analysis using the calibrated severity score (CSS), which adjusted for differences in age, intellectual abilities, and language skills across ADOS modules (Gotham et al., 2009; Jones and Lord, 2013).

2.11. Cognitive decoding analysis

To assess how predictive brain regions are associated with cognitive states, we associated maps of regression coefficients and diverse maps representing functional attributions of specific topics of cognition, which were derived from a meta-analysis using Neurosynth (Yarkoni et al., 2011). The maps contained 24 cognitive domains of sensory processing for cognition and memory-related processes (Margulies et al., 2016). Specifically, the topics included motor, eye movements, visual perception, pain, action, face, reading, semantic, multisensory, visuospatial, auditory, visual attention, language, attention, inhibition, working memory, affective, cognitive control, episodic memory, reward, autobiographical memory, verbal, emotion, and social cognition. The significance of the correlations was determined based on 1000 permutation tests.

2.12. Sensitivity analysis

a) *Different parcellation scales.* To assess the robustness of the between-group differences in the eigenvector asymmetry, we repeated the analyses with different spatial granularities of 100 and 300 parcels (Schaefer et al., 2018).
b) *Homotopic parcellation scheme.* The Schaefer atlas is an inherently asymmetric parcellation scheme (Schaefer et al., 2018), and we matched the left and right hemispheres to assess inter-hemispheric asymmetry in the main analyses. Nevertheless, we additionally generated eigenvectors using a homotopic parcellation scheme (Yan et al., 2023) and assessed similarities with the Schaefer parcellation.
c) *Head motion effect.* To ensure the validity of our findings, we additionally controlled for head motion from the eigenvectors based on the framewise displacement (Power et al., 2012) and evaluated the between-group differences in structural connectome asymmetry.

3. Results

3.1. Atypical structural connectome asymmetry in autism

To assess alterations in a compact feature set of structural connectivity in the low-dimensional manifold space in individuals with autism, we estimated cortex-wide structural connectome eigenvectors by applying nonlinear dimensionality reduction techniques to a diffusion MRI tractography-derived structural connectivity matrix (Coifman and Lafon, 2006; Vos de Wael et al., 2020). The first three eigenvectors (E1, E2, and E3) explained approximately 71.70 % of the total connectome information, where E1, E2, and E3 depicted anterior-posterior, superior-inferior, and lateral-medial axes, respectively, which reflect cortical hierarchy involved in cognitive processing and evolutionary adaptation (Fig. 1A) (Mesulam, 1998; Valk et al., 2020). Specifically, the

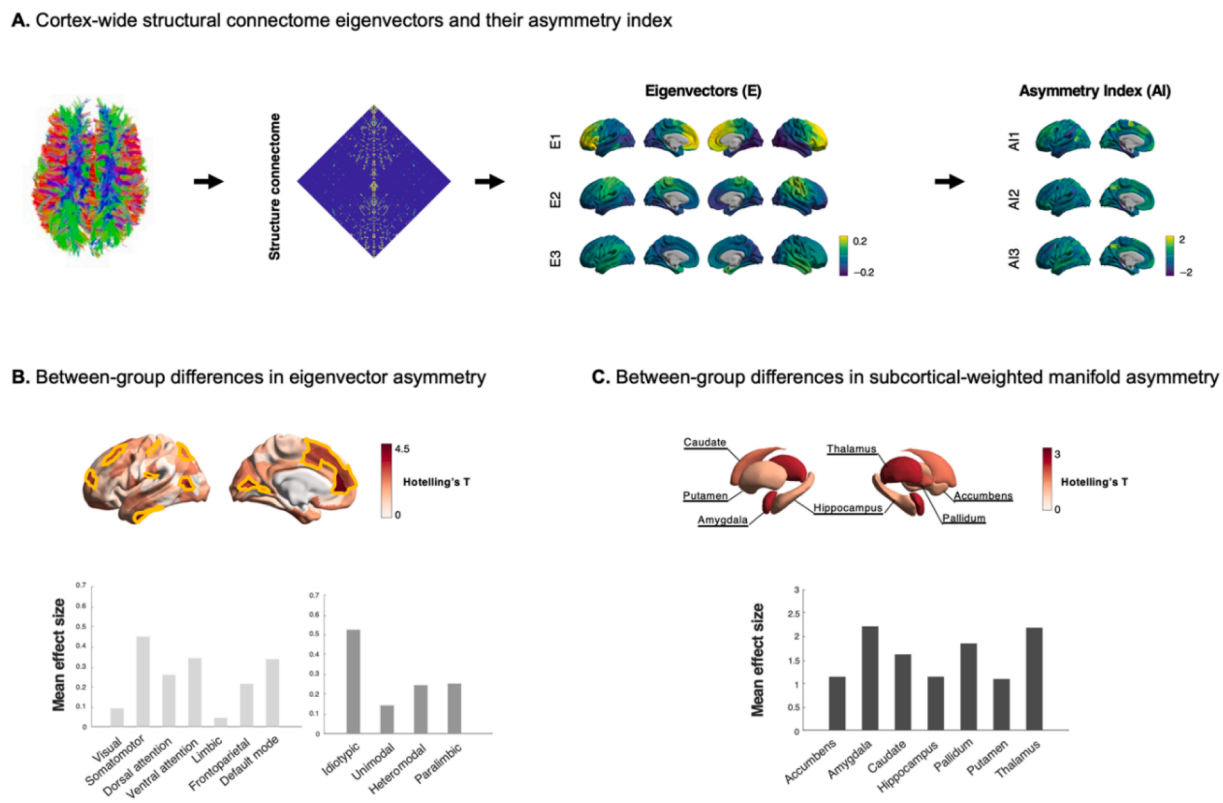

Fig. 1. Atypical structural connectome asymmetry in individuals with autism. (A) The structural connectome was estimated using diffusion MRI tractography (left). Three eigenvectors (E1, E2, and E3; middle) and the asymmetry index are shown on brain surfaces (right). (B) T-statistics of between-group differences in the asymmetry index are reported on brain surfaces, and the regions that showed significant (FDR < 0.05) effects are marked with yellow boundaries (upper). We stratified the between-group differences of the asymmetry index according to seven intrinsic function communities and four cortical hierarchical levels using bar plots (bottom). (C) The between-group differences in the subcortical-weighted manifold asymmetry. *Abbreviations:* MRI, magnetic resonance imaging; FDR, false discovery rate.

anterior-posterior axis integrates multiple cognitive control processes from sensory stimuli to perception processing (Badre and D'esposito, 2009; Goodale and Milner, 1992), the superior-inferior axis is similar to the sensory-transmodal hierarchy model (Margulies et al., 2016), and the lateral-medial axis may describe the long-range association fibers (Tanglay et al., 2022). We then calculated the asymmetry index of the structural eigenvectors and performed multivariate analysis to compare the three asymmetry maps between individuals with autism and neurotypical controls. We observed significant between-group differences in the lateral and medial visual, inferior temporal, dorsolateral and dorsomedial prefrontal, superior parietal, and somatomotor cortices (FDR < 0.05; yellow boundaries in Fig. 1B). By stratifying the effects according to seven intrinsic functional communities (Yeo et al., 2011) and a well-established model of large-scale cortical organization (Mesulam, 1998), we found the highest effects in the idiotypic regions, including the somatomotor network, followed by the default-mode regions (Fig. 1B). In addition to cortical alterations, we investigated the between-group difference effects in subcortical areas using a subcortical-weighted manifold, reflecting subcortico-cortical connectivity weighted by the eigenvectors (Park et al., 2021c). We calculated the asymmetry of this subcortical-weighted manifold and compared it between individuals with autism and neurotypical controls; however, no significant regions passed for the significance level (Fig. 1C). To assess the directionality of the asymmetry index, we stratified the averaged asymmetry index across the three eigenvectors of the regions that showed significant between-group differences in the asymmetry index between the individuals with autism and neurotypical controls (**Supplementary Fig. 1**). The inferior temporal cortex especially showed stronger asymmetry towards the right hemisphere in neurotypical controls compared to the individuals with autism, which might be related to language-related processing.

3.2. *Between-group differences in structural connectivity and network communication*

To assess the topological properties of structural connectome asymmetry in autism, we investigated between-group differences in structural connectivity that showed significant between-group differences in the asymmetry index (*i.e.,* seed regions) and seven functional networks (Yeo et al., 2011) (*i.e.,* target regions) between individuals with autism and neurotypical controls (Fig. 2A). We observed significant decreases in structural connectivity between the inferior temporal cortex and ventral attention network in individuals with autism ($p_{perm\text{-}FDR}$= 0.047; Fig. 2B). As a communication measure, we computed the navigation efficiency to compare the information transfer ability between the groups. We found significant between-group differences between the inferior temporal cortex and limbic and frontoparietal networks ($p_{perm\text{-}FDR}$= 0.031, 0.031, respectively; Fig. 2C). Specifically, individuals with autism showed decreased navigation efficiency compared to the neurotypical controls. The findings indicate that the network communication may be altered between the temporal cortex and large-scale functional brain networks, including the higher-order brain regions. Hence, the structural connectivity and communication efficiency decreased in individuals with autism, particularly in the temporal cortex.

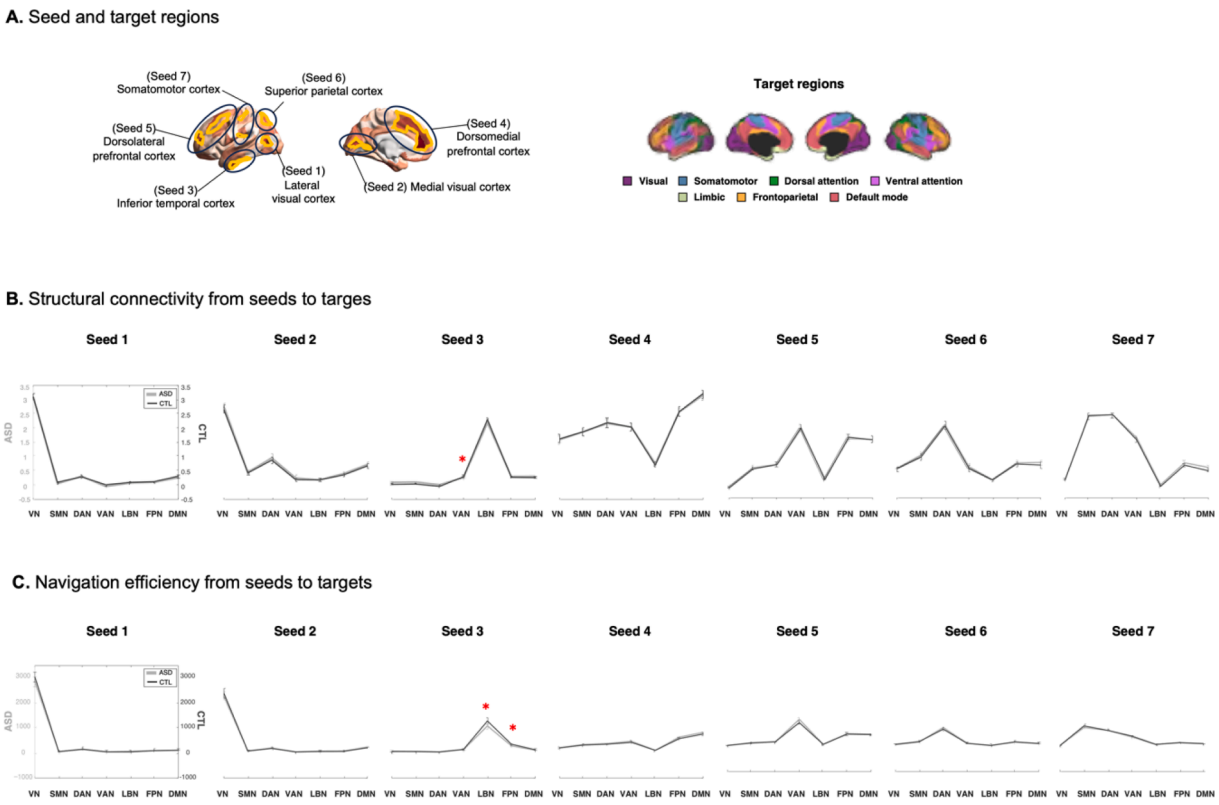

Fig. 2. Topological underpinnings of regions showing atypical structural connectome asymmetry. (A) The seed and target regions are defined. (B) Between-group differences in seed-to-target structural connectivity and (C) navigation efficiency between individuals with autism and neurotypical controls. Asterisks indicate significant differences ($p_{perm\text{-}FDR} < 0.05$). *Abbreviations:* ASD, autism spectrum disorder; CTL, control; VN, visual network; SMN, somatomotor network; DAN, dorsal attention network; VAN, ventral attention network; LBN, limbic network; FPN, frontoparietal network; DMN, default-mode network.

3.3. Send-receive communication of atypical structural connectome asymmetry

Using navigation efficiency, we investigated the send-receive network communication of regions that showed significant between-group differences in structural connectome asymmetry (Fig. 3A). We found that seed 1 (lateral visual cortex) and seed 3 (inferior temporal cortex) showed lower levels of receiving navigation efficiency in individuals with autism ($p_{perm\text{-}FDR}$= 0.039 and 0.027, respectively; Fig. 3B-C). These findings indicate that individuals with autism have altered network communication efficiency in the regions characterized by atypical structural connectome asymmetry.

3.4. Behavioral phenotypes prediction

Utilizing supervised machine learning, we predicted behavioral phenotypes described by the ADOS social cognition, communication, repetitive behavior/interest sub-scores, and a total score, and verbal and performance IQ measures and their ratio (*i.e.,* verbal/performance IQ) (Hong et al., 2022) using the asymmetry index of the three eigenvectors. We significantly predicted the ADOS total score (ICC= 0.287, p_{ICC}= 0.038; Spearman correlation coefficient [ρ]= 0.310, p_ρ = 0.059) and communication subscore (ICC= 0.308, p_{ICC}= 0.028; ρ= 0.422, p_ρ = 0.008; Fig. 4A). In addition, performance IQ (ICC= 0.186, p_{ICC}= 0.045; ρ= 0.281, p_ρ = 0.010) and IQ ratio showed significant results (ICC= 0.416, $p_{ICC} < 0.001$; ρ= 0.4457, $p_\rho < 0.001$; Fig. 4B). We additionally predicted the CSS score using subjects from the NYU site. We found a consistent pattern, although it was not significant, which might be due to the small sample size (**Supplementary Fig.2**). The degree of contribution of brain regions for predicting each score was further associated with meta-analysis maps of 24 different cognitive domains derived using Neurosynth (Margulies et al., 2016), and relations to high-level sensory and perception systems were observed (**Supplementary Fig. 3**).

3.5. Sensitivity analysis

a) *Different parcellation scales.* We generated eigenvectors based on a functionally defined atlas with 100 and 300 similarly sized parcels (Schaefer et al., 2018) and assessed between-group differences in the asymmetry index of the eigenvectors between individuals with autism and neurotypical controls. Consistent results were obtained across different spatial granularities (**Supplementary Fig. 4**).
b) *Homotopic parcellation scheme.* We repeated the analysis of generating structural connectome eigenvectors using a homotopic parcellation scheme (Yan et al., 2023). We observed that the spatial patterns of eigenvectors based on the homotopic atlas were similar to those based on the Schaefer atlas (E1: $r = 0.658$; E2: $r = 0.717$; E3: $r = 0.373$, all $p < 0.001$; **Supplementary Fig. 5**).
c) *Head motion effect.* We examined between-group differences in structural connectome asymmetry after controlling for the framewise displacement (Power et al., 2012). We found consistent results, indicating that head movements do not significantly affect perturbations in interhemispheric asymmetry in individuals with autism (**Supplementary Fig. 6**).

4. Discussion

Brain network disorganization is commonly observed in individuals with autism, and asymmetry of brain morphology has been reported in multiple studies (Floris et al., 2021; Postema et al., 2019; Sha et al., 2022). Herein, we expanded upon prior works by systematically investigating atypical structural connectome asymmetry in individuals with

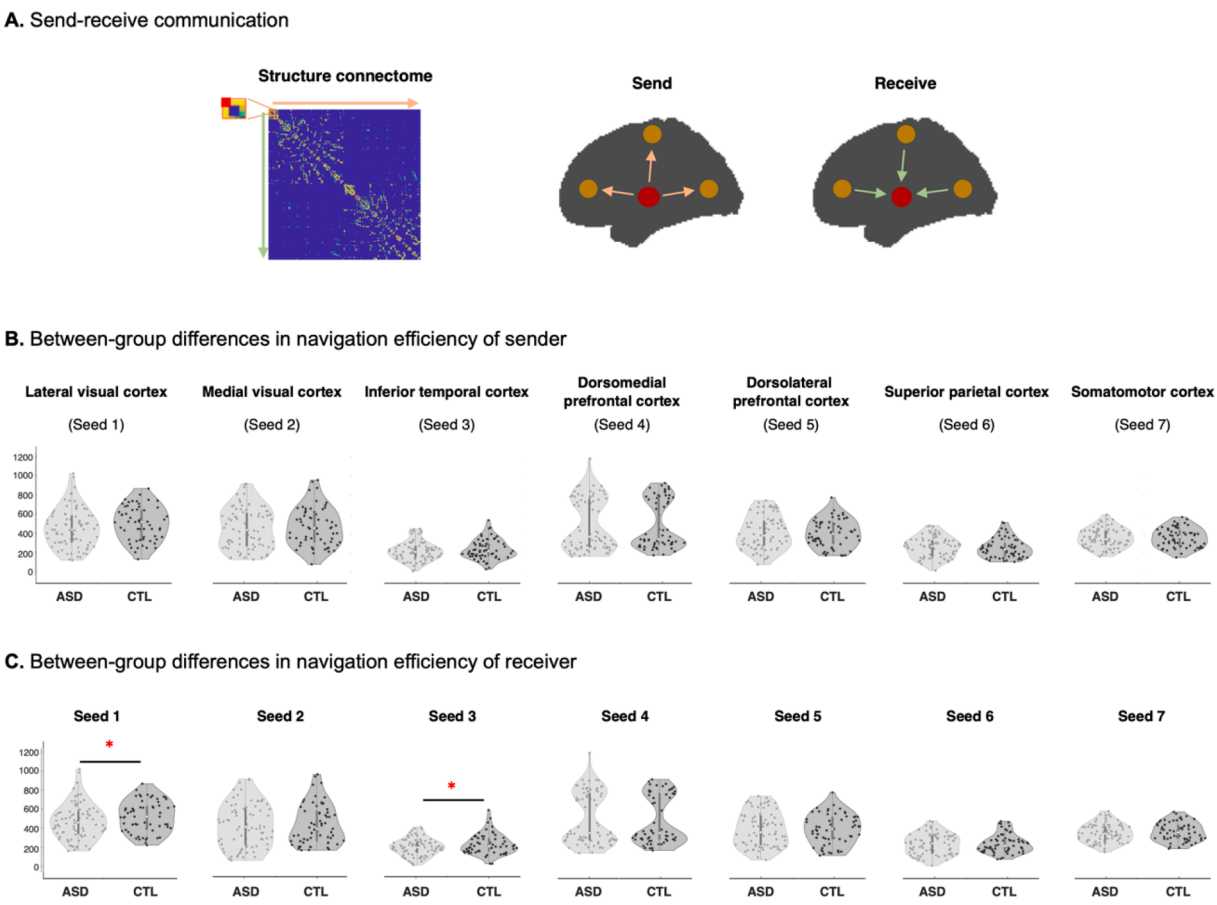

Fig. 3. Send-receive communication of the regions showing atypical structural connectome asymmetry. (A) Schema of the send-receive communication of navigation efficiency. (B) Violin plots represent the distribution of sending and (C) receiving navigation efficiency of autism and control groups for each seed. *Abbreviations:* ASD, autism spectrum disorder; CTL, control.

autism using low-dimensional representations of structural connectivity (Park et al., 2021a, 2021c). We observed alterations in the inter-hemispheric structural connectome asymmetry in the sensory, default-mode regions, particularly showing weaker asymmetry rightward in autism. Network communication analyses revealed that the inferior temporal cortex and limbic and frontoparietal regions showed reduced global network communication efficiency and decreased send-receive network navigation in the inferior temporal and lateral visual cortices in individuals with autism. Supervised machine learning indicated that the asymmetry index may serve as a marker of autism-related communication ability and intelligence. Our findings provide insights into understanding atypical structural connectome asymmetry and network communication topology in individuals with autism.

We utilized dimensionality reduction techniques to represent cortex-wide structural connectivity with a set of macroscale eigenvectors. The selected three eigenvectors showed anterior-posterior, superior-inferior, and lateral-medial axes, consistent with the findings of previous studies (Hagmann et al., 2008; Park et al., 2021a, 2021c; Valk et al., 2020). The anterior-posterior axis is a key structure of cortical organization established in non-human primates and the human brain (Hagmann et al., 2008; Mesulam, 1998; Paquola et al., 2020). This axis consists of the rostrocaudal axis in the prefrontal cortex, which integrates multiple cognitive control processes, particularly action coupled with premotor processes (Badre and D'esposito, 2009; Braga et al., 2017; Nachev et al., 2008), and the ventral visual stream spans from the primary visual cortex to the ventral areas in the occipital and temporal cortices that implement perception processing (Borghesani et al., 2016; Goodale and Milner, 1992; Grill-Spector and Malach, 2004; Takemura et al., 2016). The superior-inferior axis resembled an established model of the sensory-transmodal hierarchy (Margulies et al., 2016), which expands from the sensorimotor area with higher myelination to heteromodal association areas with lower myelination. The lateral-medial axis is relatively under-investigated. This axis may represent long-range association fibers, such as the cingulum bundle originating from the precuneus to the orbitofrontal cortex and parahippocampal gyrus and middle longitudinal fasciculus fibers that stem from the precuneus to the lateral temporal pole, which was defined from a human *post-mortem* study (Tanglay et al., 2022).

Our findings highlighted that the principal axes of structural connectivity showed atypical asymmetry in individuals with autism, particularly in the default-mode and sensory regions. A previous study based on the ENIGMA dataset found network-level asymmetry in cortical thickness-based structural covariance in the fusiform gyrus and superior and middle frontal cortices of individuals with autism (Sha et al., 2022). Another study observed brain asymmetry in language processing-related sensory and transmodal regions in individuals with autism (Herbert et al., 2005). At the microscale, individuals with autism show less clear laminar differentiation between cortical layers IV and V (Oblak et al., 2011b) and reduced neurotransmitter receptor binding density in the posterior cingulate cortex (Oblak et al., 2011a). Biophysical simulations have revealed that excitation/inhibition is related to atypical structural connectomes in autism, particularly in somatosensory and default-mode systems (Park et al., 2021c). These studies complement our findings that default-mode and sensory regions are crucial in autism at multiple scales, from macroscopic connectomics to microscale cytoarchitecture and neurotransmitters. Expanding on previous studies, we offer perspectives on atypical structural connectome

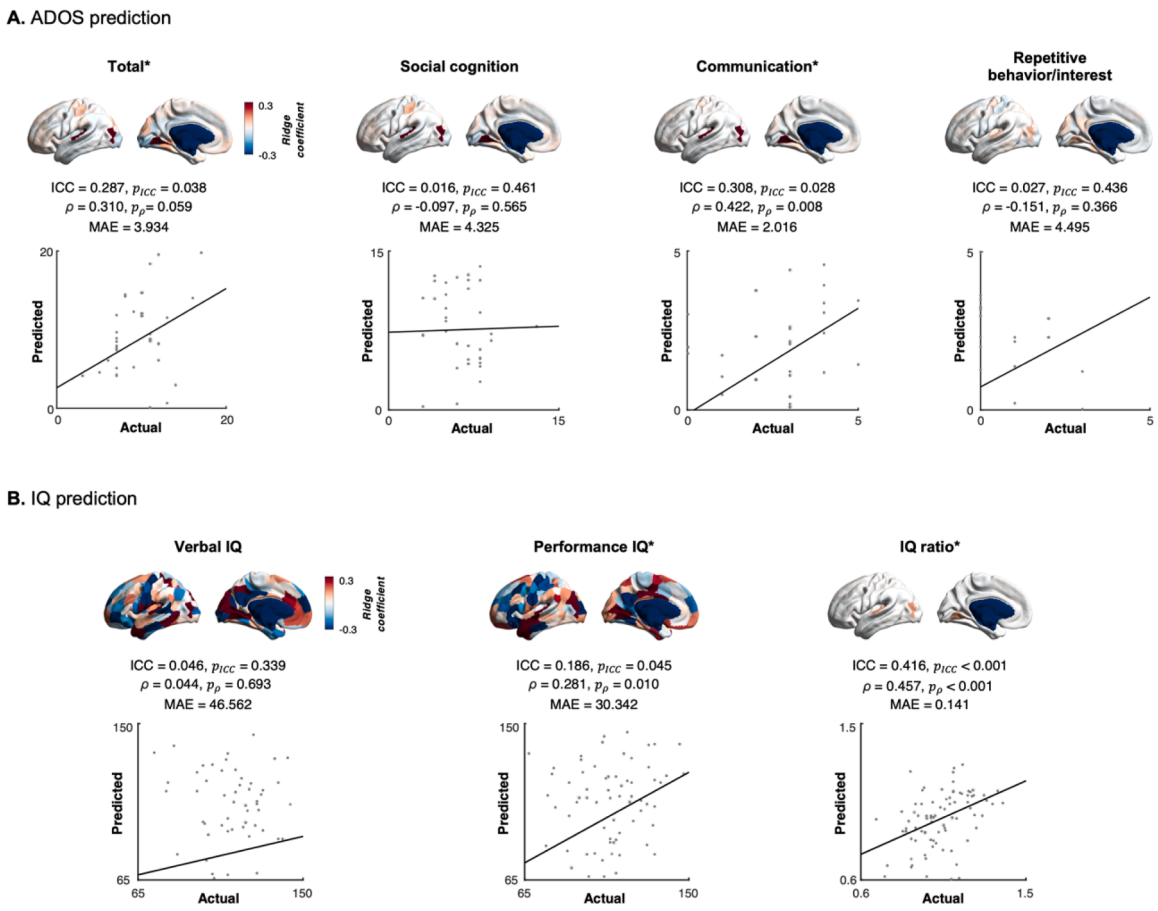

Fig. 4. Prediction of behavioral phenotypes using structural connectome asymmetry. (A) We calculated Spearman correlations between the actual and predicted scores of ADOS total, social cognition, communication, and repetitive behavior/interest scores. The coefficients of ridge regression are reported on brain surfaces. (B) We predicted verbal and performance IQ as well as their ratio. *Abbreviations:* ADOS, Autism Diagnostic Observation Schedule; IQ, intelligence quotient; ICC, intra-class correlation coefficient; ρ, Spearman correlation coefficient; MAE, mean absolute error.

asymmetry in autism.

Notably, our findings exhibited that the asymmetry in the eigenvectors was reduced in individuals with autism, which was more lateralized toward the right hemisphere in the neurotypical controls. The findings complement prior work that individuals with autism showed reduced brain asymmetry, resulting in atypical developmental trajectories in language and cognitive control systems (Dougherty et al., 2016; Herbert et al., 2002), and may support a hypothesis that the atypical brain asymmetry in autism might be due to the reduced hemispheric specialization in brain structure (Floris et al., 2021). However, the interpretation needs caution because whether the brain asymmetry in autism is due to strengthening or weakening of connectivity requires more in-depth exploration using a large-scale dataset. Furthermore, we investigated the underlying connectional topology of inter-hemispheric asymmetry in autism using network communication based on a feature called network navigation, which measures the efficiency of transverse information between different brain regions based on the greedy routing algorithm (Seguin et al., 2019, 2018). The significance of group difference in receive of navigation efficiency was observed in lateral visual and inferior temporal cortices. Studies on human and non-human primates have demonstrated that the temporal cortex is involved in higher-order sensory processing, such as language, auditory, and visual perception, and encoding of memory and emotion (Perrett et al., 1992, 1984; Puce et al., 1998). Alterations in the network communication in the temporal cortex may be associated with abnormal language skills and perceptions in individuals with autism. Moreover, atypical incoming and outgoing network communication in the lateral visual cortex and inferior temporal in individuals with autism indicates susceptibility to the disease. Taken together, the atypical inter-hemispheric asymmetry in structural eigenvectors may be associated with an altered routing network communication in individuals with autism.

As a final analysis, we adopted supervised machine learning with cross-validation and regularization to predict the symptoms and intelligence of individuals with autism using the asymmetry index of structural connectivity. We found that asymmetry features are associated with atypical communication skills as well as performance IQ and IQ ratio, which may depend on altered cognitive and social development (Chiang et al., 2008; Wilkinson, 1998). Although more elaborate methodological approaches need to be considered to fully explain ongoing autistic symptoms and intellectual development, our findings provide insights into brain-behavior relationships in individuals with autism.

In this study, we systemically studied atypical structural connectome asymmetry in individuals with autism, investigated its topological underpinnings via network communication measures, and further stated the possibility of asymmetry as a marker for autism. Specifically, we identified large-scale network-level imaging features significantly associated with symptom severity and intelligence in individuals with autism, which may help better understand the underlying network communication mechanisms of the brain related to autistic traits. Furthermore, our findings provide insights into understanding the links across whole-brain structural connectome asymmetry, network communication mechanisms, and behavioral phenotypes in individuals with autism. Together, our results may advance our knowledge

regarding the brain mechanisms of autism.

Code availability

The codes for eigenvector generation are available at https://github.com/MICA-MNI/BrainSpace, codes for calculating network communication measures are available at https://sites.google.com/site/bctnet/, and codes for statistical analyses are available at https://github.com/MICA-MNI/ENIGMA.

CRediT authorship contribution statement

Seulki Yoo: Writing – original draft, Visualization, Validation, Software, Methodology, Investigation, Formal analysis, Conceptualization. **Yurim Jang:** Writing – review & editing, Methodology, Investigation, Formal analysis. **Seok-Jun Hong:** Writing – review & editing, Resources, Funding acquisition. **Hyunjin Park:** Writing – review & editing, Resources, Funding acquisition. **Sofie L. Valk:** Writing – review & editing, Resources, Conceptualization. **Boris C. Bernhardt:** Writing – review & editing, Software, Resources, Conceptualization. **Bo-yong Park:** Writing – original draft, Visualization, Validation, Supervision, Software, Resources, Project administration, Methodology, Investigation, Funding acquisition, Formal analysis, Data curation, Conceptualization.

Declaration of competing interest

All authors declare no conflicts of interest.

Data availability

I have shared the link to my data/code at the Attach File step.

Funding

Bo-yong Park received funding from the National Research Foundation of Korea (NRF-2021R1F1A1052303; NRF-2022R1A5A7033499), Institute for Information and Communications Technology Planning and Evaluation (IITP) funded by the Korea Government (MSIT) (No. 2022–0-00448, Deep Total Recall: Continual Learning for Human-Like Recall of Artificial Neural Networks; No. RS-2022–00155915, Artificial Intelligence Convergence Innovation Human Resources Development (Inha University); No. 2021–0-02068, Artificial Intelligence Innovation Hub), and Institute for Basic Science (IBS-R015-D1).

Supplementary materials

Supplementary material associated with this article can be found, in the online version, at doi:10.1016/j.neuroimage.2024.120534.

References

Avena-Koenigsberger, A., Misic, B., Sporns, O., 2018. Communication dynamics in complex brain networks. Nat. Rev. Neurosci. 19, 17–33.
Avena-Koenigsberger, A., Yan, X., Kolchinsky, A., van den Heuvel, M.P., Hagmann, P., Sporns, O., 2019. A spectrum of routing strategies for brain networks. PLoS Comput. Biol. 15, e1006833.
Badre, D., D'esposito, M., 2009. Is the rostro-caudal axis of the frontal lobe hierarchical? Nat. Rev. Neurosci. 10, 659–669.
Baio, J., Wiggins, L., Christensen, D.L., Maenner, M.J., Daniels, J., Warren, Z., Kurzius-Spencer, M., Zahorodny, W., Rosenberg, C.R., White, T., 2018. Prevalence of autism spectrum disorder among children aged 8 years—Autism and developmental disabilities monitoring network, 11 sites, United States, 2014. MMWR Surveill. Summ. 67, 1.
Balathay, D., Narasimhan, U., Belo, D., Anandan, K., 2023. Quantitative assessment of cognitive profile and brain asymmetry in the characterization of autism spectrum in children: a task-based EEG study. In: Proceedings of the Institution of Mechanical Engineers, Part H: Journal of Engineering in Medicine, 237, pp. 653–665.
Benjamini, Y., Hochberg, Y., 1995. Controlling the false discovery rate: a practical and powerful approach to multiple testing. J. R. Stat. Soc. Series B Stat. Methodol. 57, 289–300.
Bernasconi, N., Bernasconi, A., Caramanos, Z., Antel, S., Andermann, F., Arnold, D.L., 2003. Mesial temporal damage in temporal lobe epilepsy: a volumetric MRI study of the hippocampus, amygdala and parahippocampal region. Brain 126, 462–469.
Betzel, R.F., Griffa, A., Hagmann, P., Mišić, B., 2019. Distance-dependent consensus thresholds for generating group-representative structural brain networks. Network Neurosci. 3, 475–496.
Borghesani, V., Pedregosa, F., Buiatti, M., Amadon, A., Eger, E., Piazza, M., 2016. Word meaning in the ventral visual path: a perceptual to conceptual gradient of semantic coding. Neuroimage 143, 128–140.
Braga, R.M., Hellyer, P.J., Wise, R.J., Leech, R., 2017. Auditory and visual connectivity gradients in frontoparietal cortex. Hum. Brain Mapp. 38, 255–270.
Cerliani, L., Mennes, M., Thomas, R.M., Di Martino, A., Thioux, M., Keysers, C., 2015. Increased functional connectivity between subcortical and cortical resting-state networks in autism spectrum disorder. JAMA Psychiatry 72, 767–777.
Chiang, C.H., Soong, W.T., Lin, T.L., Rogers, S.J., 2008. Nonverbal communication skills in young children with autism. J. Autism Dev. Disord. 38, 1898–1906.
Christensen, D.L., Braun, K.V.N., Baio, J., Bilder, D., Charles, J., Constantino, J.N., Daniels, J., Durkin, M.S., Fitzgerald, R.T., Kurzius-Spencer, M., 2018. Prevalence and characteristics of autism spectrum disorder among children aged 8 years—Autism and developmental disabilities monitoring network, 11 sites, United States, 2012. MMWR Surveill. Summ. 65, 1.
Christiaens, D., Reisert, M., Dhollander, T., Sunaert, S., Suetens, P., Maes, F., 2015. Global tractography of multi-shell diffusion-weighted imaging data using a multi-tissue model. Neuroimage 123, 89–101.
Chung, M.K., Worsley, K.J., Nacewicz, B.M., Dalton, K.M., Davidson, R.J., 2010. General multivariate linear modeling of surface shapes using SurfStat. Neuroimage 53, 491–505.
Coifman, R.R., Lafon, S., 2006. Diffusion maps. Appl. Comput. Harmon. Anal. 21, 5–30.
Dale, A.M., Fischl, B., Sereno, M.I., 1999. Cortical surface-based analysis: I. Segmentation and surface reconstruction. Neuroimage 9, 179–194.
Di Martino, A., O'connor, D., Chen, B., Alaerts, K., Anderson, J.S., Assaf, M., Balsters, J. H., Baxter, L., Beggiato, A., Bernaerts, S., 2017. Enhancing studies of the connectome in autism using the autism brain imaging data exchange II. Sci. Data 4, 1–15.
Di Martino, A., Yan, C.G., Li, Q., Denio, E., Castellanos, F.X., Alaerts, K., Anderson, J.S., Assaf, M., Bookheimer, S.Y., Dapretto, M., 2014. The autism brain imaging data exchange: towards a large-scale evaluation of the intrinsic brain architecture in autism. Mol. Psychiatry 19, 659–667.
Dougherty, C.C., Evans, D.W., Katuwal, G.J., Michael, A.M., 2016. Asymmetry of fusiform structure in autism spectrum disorder: trajectory and association with symptom severity. Mol. Autism 7, 1–11.
Fischl, B., Liu, A., Dale, A.M., 2001. Automated manifold surgery: constructing geometrically accurate and topologically correct models of the human cerebral cortex. IEEE Trans. Med. Imaging 20, 70–80.
Fischl, B., Sereno, M.I., Dale, A.M., 1999a. Cortical surface-based analysis: II: inflation, flattening, and a surface-based coordinate system. Neuroimage 9, 195–207.
Fischl, B., Sereno, M.I., Tootell, R.B., Dale, A.M., 1999b. High-resolution intersubject averaging and a coordinate system for the cortical surface. Hum. Brain Mapp. 8, 272–284.
Floris, D.L., Wolfers, T., Zabihi, M., Holz, N.E., Zwiers, M.P., Charman, T., Tillmann, J., Ecker, C., Dell'Acqua, F., Banaschewski, T., 2021. Atypical brain asymmetry in autism—A candidate for clinically meaningful stratification. Biol. Psychiatry 6, 802–812.
Fornito, A., Zalesky, A., Bullmore, E., 2016. Fundamentals of Brain Network Analysis. Academic Press.
Goñi, J., Van Den Heuvel, M.P., Avena-Koenigsberger, A., Velez de Mendizabal, N., Betzel, R.F., Griffa, A., Hagmann, P., Corominas-Murtra, B., Thiran, J.P., Sporns, O., 2014. Resting-brain functional connectivity predicted by analytic measures of network communication. In: Proceedings of the National Academy of Sciences, 111, pp. 833–838.
Goodale, M.A., Milner, A.D., 1992. Separate visual pathways for perception and action. Trends Neurosci. 15, 20–25.
Gotham, K., Pickles, A., Lord, C., 2009. Standardizing ADOS scores for a measure of severity in autism spectrum disorders. J. Autism Dev. Disord. 39, 693–705.
Grill-Spector, K., Malach, R., 2004. The human visual cortex. Annu. Rev. Neurosci. 27, 649–677.
Guo, X., Simas, T., Lai, M.C., Lombardo, M.V., Chakrabarti, B., Ruigrok, A.N., Bullmore, E.T., Baron-Cohen, S., Chen, H., Suckling, J., 2019. Enhancement of indirect functional connections with shortest path length in the adult autistic brain. Hum. Brain Mapp. 40, 5354–5369.
Haak, K.V., Beckmann, C.F., 2020. Understanding brain organisation in the face of functional heterogeneity and functional multiplicity. Neuroimage 220, 117061.
Haak, K.V., Marquand, A.F., Beckmann, C.F., 2018. Connectopic mapping with resting-state fMRI. Neuroimage 170, 83–94.
Hagmann, P., Cammoun, L., Gigandet, X., Meuli, R., Honey, C.J., Wedeen, V.J., Sporns, O., 2008. Mapping the structural core of human cerebral cortex. PLoS Biol. 6, e159.
Herbert, M.R., Harris, G.J., Adrien, K.T., Ziegler, D.A., Makris, N., Kennedy, D.N., Lange, N.T., Chabris, C.F., Bakardjiev, A., Hodgson, J., 2002. Abnormal asymmetry in language association cortex in autism. Ann. Neurol. 52, 588–596.
Herbert, M.R., Ziegler, D.A., Deutsch, C., O'Brien, L.M., Kennedy, D.N., Filipek, P., Bakardjiev, A., Hodgson, J., Takeoka, M., Makris, N., 2005. Brain asymmetries in autism and developmental language disorder: a nested whole-brain analysis. Brain 128, 213–226.

Hong, S.J., Mottron, L., Park, B.-y., Benkarim, O., Valk, S.L., Paquola, C., Larivière, S., Vos de Wael, R., Degré-Pelletier, J., Soulieres, I., Ramphal, B., Margolis, A., Milham, M., Di Martino, A., Bernhardt, B.C., 2022. A convergent structure–function substrate of cognitive imbalances in autism. Cereb. Cortex.
Hong, S.J., Vos de Wael, R., Bethlehem, R.A., Lariviere, S., Paquola, C., Valk, S.L., Milham, M.P., Di Martino, A., Margulies, D.S., Smallwood, J., 2019. Atypical functional connectome hierarchy in autism. Nat. Commun. 10, 1–13.
Huntenburg, J.M., Bazin, P.L., Margulies, D.S., 2018. Large-scale gradients in human cortical organization. Trends Cogn. Sci. (Regul. Ed.) 22, 21–31.
Jeurissen, B., Tournier, J.D., Dhollander, T., Connelly, A., Sijbers, J., 2014. Multi-tissue constrained spherical deconvolution for improved analysis of multi-shell diffusion MRI data. Neuroimage 103, 411–426.
Jones, R.M., Lord, C., 2013. Diagnosing autism in neurobiological research studies. Behav. Brain Res. 251, 113–124.
Jou, R.J., Jackowski, A.P., Papademetris, X., Rajeevan, N., Staib, L.H., Volkmar, F.R., 2011. Diffusion tensor imaging in autism spectrum disorders: preliminary evidence of abnormal neural connectivity. Australian New Zealand J. Psychiatry 45, 153–162.
Khundrakpam, B.S., Lewis, J.D., Kostopoulos, P., Carbonell, F., Evans, A.C., 2017. Cortical thickness abnormalities in autism spectrum disorders through late childhood, adolescence, and adulthood: a large-scale MRI study. Cereb. Cortex 27, 1721–1731.
Kong, X.Z., Mathias, S.R., Guadalupe, T., Group, E.L.W., Glahn, D.C., Franke, B., Crivello, F., Tzourio-Mazoyer, N., Fisher, S.E., Thompson, P.M., 2018. Mapping cortical brain asymmetry in 17,141 healthy individuals worldwide via the ENIGMA Consortium. In: Proceedings of the National Academy of Sciences, 115, pp. E5154–E5163.
Langs, G., Golland, P., Ghosh, S.S., 2015. Predicting activation across individuals with resting-state functional connectivity based multi-atlas label fusion. In: International Conference on Medical Image Computing and Computer-Assisted Intervention. Springer, pp. 313–320.
Lee, E., Lee, J., Kim, E., 2017. Excitation/inhibition imbalance in animal models of autism spectrum disorders. Biol. Psychiatry 81, 838–847.
Lewis, J.D., Evans, A., Pruett, J., Botteron, K., Zwaigenbaum, L., Estes, A., Gerig, G., Collins, L., Kostopoulos, P., McKinstry, R., 2014. Network inefficiencies in autism spectrum disorder at 24 months. Transl. Psychiatry 4, e388. -e388.
Lord, C., Risi, S., Lambrecht, L., Cook, E.H., Leventhal, B.L., DiLavore, P.C., Pickles, A., Rutter, M., 2000. The Autism Diagnostic Observation Schedule—Generic: a standard measure of social and communication deficits associated with the spectrum of autism. J. Autism Dev. Disord. 30, 205–223.
Lord, C., Rutter, M., Le Couteur, A., 1994. Autism Diagnostic Interview-Revised: a revised version of a diagnostic interview for caregivers of individuals with possible pervasive developmental disorders. J. Autism Dev. Disord. 24, 659–685.
Margulies, D.S., Ghosh, S.S., Goulas, A., Falkiewicz, M., Huntenburg, J.M., Langs, G., Bezgin, G., Eickhoff, S.B., Castellanos, F.X., Petrides, M., 2016. Situating the default-mode network along a principal gradient of macroscale cortical organization. In: Proceedings of the National Academy of Sciences, 113, pp. 12574–12579.
McDonald, G.C., 2009. Ridge regression. Wiley Interdiscip. Rev. Comput. Stat. 1, 93–100.
Mesulam, M.M., 1998. From sensation to cognition. Brain 121, 1013–1052.
Mottron, L., Dawson, M., Soulières, I., Hubert, B., Burack, J., 2006. Enhanced perceptual functioning in autism: an update, and eight principles of autistic perception. J. Autism Dev. Disord. 36, 27–43.
Nachev, P., Kennard, C., Husain, M., 2008. Functional role of the supplementary and pre-supplementary motor areas. Nat. Rev. Neurosci. 9, 856–869.
Nair, A., Treiber, J.M., Shukla, D.K., Shih, P., Müller, R.A., 2013. Impaired thalamocortical connectivity in autism spectrum disorder: a study of functional and anatomical connectivity. Brain 136, 1942–1955.
Nelson, S.B., Valakh, V., 2015. Excitatory/inhibitory balance and circuit homeostasis in autism spectrum disorders. Neuron 87, 684–698.
Nunes, A.S., Peatfield, N., Vakorin, V., Doesburg, S.M., 2019. Idiosyncratic organization of cortical networks in autism spectrum disorder. Neuroimage 190, 182–190.
Oblak, A.L., Gibbs, T.T., Blatt, G.J., 2011a. Reduced GABAA receptors and benzodiazepine binding sites in the posterior cingulate cortex and fusiform gyrus in autism. Brain Res. 1380, 218–228.
Oblak, A.L., Rosene, D.L., Kemper, T.L., Bauman, M.L., Blatt, G.J., 2011b. Altered posterior cingulate cortical cytoarchitecture, but normal density of neurons and interneurons in the posterior cingulate cortex and fusiform gyrus in autism. Autism Res. 4, 200–211.
Okada, N., Fukunaga, M., Yamashita, F., Koshiyama, D., Yamamori, H., Ohi, K., Yasuda, Y., Fujimoto, M., Watanabe, Y., Yahata, N., 2016. Abnormal asymmetries in subcortical brain volume in schizophrenia. Mol. Psychiatry 21, 1460–1466.
Paquola, C., Seidlitz, J., Benkarim, O., Royer, J., Klimes, P., Bethlehem, R.A., Larivière, S., Vos de Wael, R., Rodríguez-Cruces, R., Hall, J.A., 2020. A multi-scale cortical wiring space links cellular architecture and functional dynamics in the human brain. PLoS Biol. 18, e3000979.
Paquola, C., Vos De Wael, R., Wagstyl, K., Bethlehem, R.A., Hong, S.J., Seidlitz, J., Bullmore, E.T., Evans, A.C., Misic, B., Margulies, D.S., 2019. Microstructural and functional gradients are increasingly dissociated in transmodal cortices. PLoS Biol. 17, e3000284.
Park, B.-y., Bethlehem, R.A., Paquola, C., Larivière, S., Rodríguez-Cruces, R., de Wael, R. V., Bullmore, E.T., Bernhardt, B.C., 2021a. An expanding manifold in transmodal regions characterizes adolescent reconfiguration of structural connectome organization. eLifeeLife 10.
Park, B.-y., de Wael, R.V., Paquola, C., Larivière, S., Benkarim, O., Royer, J., Tavakol, S., Cruces, R.R., Li, Q., Valk, S.L., 2021b. Signal diffusion along connectome gradients and inter-hub routing differentially contribute to dynamic human brain function. Neuroimage 224, 117429.
Park, B.-y., Hong, S.J., Valk, S.L., Paquola, C., Benkarim, O., Bethlehem, R.A., Di Martino, A., Milham, M.P., Gozzi, A., Yeo, B., 2021c. Differences in subcortico-cortical interactions identified from connectome and microcircuit models in autism. Nat. Commun. 12, 1–15.
Park, B.-y., Vos de Wael, R., Paquola, C., Larivière, S., Benkarim, O., Royer, J., Tavakol, S., Cruces, R.R., Li, Q., Valk, S.L., 2021d. Signal diffusion along connectome gradients and inter-hub routing differentially contribute to dynamic human brain function. Neuroimage 224, 117429.
Patenaude, B., Smith, S.M., Kennedy, D.N., Jenkinson, M., 2011. A Bayesian model of shape and appearance for subcortical brain segmentation. Neuroimage 56, 907–922.
Perrett, D.I., Hietanen, J.K., Oram, M.W., Benson, P.J., 1992. Organization and functions of cells responsive to faces in the temporal cortex. Philosophical transactions of the royal society of London. Series B: Biol. Sci. 335, 23–30.
Perrett, D.I., Smith, P., Potter, D.D., Mistlin, A., Head, A., Milner, A., Jeeves, M., 1984. Neurones responsive to faces in the temporal cortex: studies of functional organization, sensitivity to identity and relation to perception. Hum. Neurobiol. 3, 197–208.
Pinto, D., Martins, R., Macedo, A., Castelo Branco, M., Valente Duarte, J., Madeira, N., 2023. Brain Hemispheric Asymmetry in Schizophrenia and Bipolar Disorder. J. Clin. Med. 12, 3421.
Postema, M.C., Hoogman, M., Ambrosino, S., Asherson, P., Banaschewski, T., Bandeira, C.E., Baranov, A., Bau, C.H., Baumeister, S., Baur-Streubel, R., 2021. Analysis of structural brain asymmetries in attention-deficit/hyperactivity disorder in 39 datasets. J. Child Psychol. Psychiatry 62, 1202–1219.
Postema, M.C., Van Rooij, D., Anagnostou, E., Arango, C., Auzias, G., Behrmann, M., Calderoni, S., Calvo, R., Daly, E., Deruelle, C., 2019. Altered structural brain asymmetry in autism spectrum disorder in a study of 54 datasets. Nat. Commun. 10, 1–12.
Power, J.D., Barnes, K.A., Snyder, A.Z., Schlaggar, B.L., Petersen, S.E., 2012. Spurious but systematic correlations in functional connectivity MRI networks arise from subject motion. Neuroimage 59, 2142–2154.
Puce, A., Allison, T., Bentin, S., Gore, J.C., McCarthy, G., 1998. Temporal cortex activation in humans viewing eye and mouth movements. J. Neurosci. 18, 2188–2199.
Sarica, A., Vasta, R., Novellino, F., Vaccaro, M.G., Cerasa, A., Quattrone, A., Initiative, A. s.D.N., 2018. MRI asymmetry index of hippocampal subfields increases through the continuum from the mild cognitive impairment to the Alzheimer's disease. Front. Neurosci. 12, 576.
Schaefer, A., Kong, R., Gordon, E.M., Laumann, T.O., Zuo, X.N., Holmes, A.J., Eickhoff, S. B., Yeo, B.T., 2018. Local-global parcellation of the human cerebral cortex from intrinsic functional connectivity MRI. Cereb. Cortex 28, 3095–3114.
Ségonne, F., Pacheco, J., Fischl, B., 2007. Geometrically accurate topology-correction of cortical surfaces using nonseparating loops. IEEE Trans. Med. Imaging 26, 518–529.
Seguin, C., Razi, A., Zalesky, A., 2019. Inferring neural signalling directionality from undirected structural connectomes. Nat. Commun. 10, 1–13.
Seguin, C., Sporns, O., Zalesky, A., Calamante, F., 2022. Network communication models narrow the gap between the modular organization of structural and functional brain networks. Neuroimage 257, 119323.
Seguin, C., Van Den Heuvel, M.P., Zalesky, A., 2018. Navigation of brain networks. In: Proceedings of the National Academy of Sciences, 115, pp. 6297–6302.
Sha, Z., Van Rooij, D., Anagnostou, E., Arango, C., Auzias, G., Behrmann, M., Bernhardt, B., Bolte, S., Busatto, G.F., Calderoni, S., 2022. Subtly altered topological asymmetry of brain structural covariance networks in autism spectrum disorder across 43 datasets from the ENIGMA consortium. Mol. Psychiatry 27, 2114–2125.
Smith, R.E., Tournier, J.D., Calamante, F., Connelly, A., 2012. Anatomically-constrained tractography: improved diffusion MRI streamlines tractography through effective use of anatomical information. Neuroimage 62, 1924–1938.
Smith, R.E., Tournier, J.D., Calamante, F., Connelly, A., 2015. SIFT2: enabling dense quantitative assessment of brain white matter connectivity using streamlines tractography. Neuroimage 119, 338–351.
Sohal, V.S., Rubenstein, J.L., 2019. Excitation-inhibition balance as a framework for investigating mechanisms in neuropsychiatric disorders. Mol. Psychiatry 24, 1248–1257.
Takemura, H., Rokem, A., Winawer, J., Yeatman, J.D., Wandell, B.A., Pestilli, F., 2016. A major human white matter pathway between dorsal and ventral visual cortex. Cereb. Cortex 26, 2205–2214.
Tanglay, O., Young, I.M., Dadario, N.B., Briggs, R.G., Fonseka, R.D., Dhanaraj, V., Hormovas, J., Lin, Y.H., Sughrue, M.E., 2022. Anatomy and white-matter connections of the precuneus. Brain Imaging Behav. 16, 574–586.
Tenenbaum, J.B., Silva, V.d., Langford, J.C., 2000. A global geometric framework for nonlinear dimensionality reduction. Science 290, 2319–2323.
Tournier, J.D., Smith, R., Raffelt, D., Tabbara, R., Dhollander, T., Pietsch, M., Christiaens, D., Jeurissen, B., Yeh, C.H., Connelly, A., 2019. MRtrix3: a fast, flexible and open software framework for medical image processing and visualisation. Neuroimage 202, 116137.
Tournier, J.D., Calamante, F., Connelly, A., 2010. Improved probabilistic streamlines tractography by 2nd order integration over fibre orientation distributions. In: Proceedings of the international society for magnetic resonance in medicine. John Wiley & Sons, Inc, New Jersey, USA.
Tournier, J.D., Calamante, F., Connelly, A., 2012. MRtrix: diffusion tractography in crossing fiber regions. Int. J. Imaging Syst. Technol. 22, 53–66.
Valk, S.L., Di Martino, A., Milham, M.P., Bernhardt, B.C., 2015. Multicenter mapping of structural network alterations in autism. Hum. Brain Mapp. 36, 2364–2373.
Valk, S.L., Xu, T., Margulies, D.S., Masouleh, S.K., Paquola, C., Goulas, A., Kochunov, P., Smallwood, J., Yeo, B.T., Bernhardt, B.C., 2020. Shaping brain structure: genetic and

phylogenetic axes of macroscale organization of cortical thickness. Sci. Adv. 6, eabb3417.
Van Rooij, D., Anagnostou, E., Arango, C., Auzias, G., Behrmann, M., Busatto, G.F., Calderoni, S., Daly, E., Deruelle, C., Di Martino, A., 2018. Cortical and subcortical brain morphometry differences between patients with autism spectrum disorder and healthy individuals across the lifespan: results from the ENIGMA ASD Working Group. Am. J. Psychiatry 175, 359–369.
Vázquez-Rodríguez, B., Suárez, L.E., Markello, R.D., Shafiei, G., Paquola, C., Hagmann, P., Van Den Heuvel, M.P., Bernhardt, B.C., Spreng, R.N., Misic, B., 2019. Gradients of structure–function tethering across neocortex. In: Proceedings of the National Academy of Sciences, 116, pp. 21219–21227.
Vézquez-Rodríguez, B., Liu, Z.Q., Hagmann, P., Misic, B., 2020. Signal propagation via cortical hierarchies. Network Neurosci. 4, 1072–1090.
Von Luxburg, U., 2007. A tutorial on spectral clustering. Stat. Comput. 17, 395–416.
Vos de Wael, R., Benkarim, O., Paquola, C., Lariviere, S., Royer, J., Tavakol, S., Xu, T., Hong, S.J., Langs, G., Valk, S., 2020. BrainSpace: a toolbox for the analysis of macroscale gradients in neuroimaging and connectomics datasets. Commun. Biol. 3, 1–10.
Wang, B., Yang, L., Yan, W., An, W., Xiang, J., Li, D., 2023. Brain asymmetry: a novel perspective on hemispheric network. Brain Sci. Adv. 9, 56–77.
Wilkinson, K.M., 1998. Profiles of language and communication skills in autism. Ment. Retard. Dev. Disabil. Res. Rev. 4, 73–79.
Worsley, K.J., Taylor, J., Carbonell, F., Chung, M., Duerden, E., Bernhardt, B., Lyttelton, O., Boucher, M., Evans, A., 2009. A Matlab toolbox for the statistical analysis of univariate and multivariate surface and volumetric data using linear mixed effects models and random field theory. In: Proceedings of the NeuroImage Organisation for Human Brain Mapping 2009 Annual Meeting, p. S102.
Yan, X., Kong, R., Xue, A., Yang, Q., Orban, C., An, L., Holmes, A.J., Qian, X., Chen, J., Zuo, X.N., 2023. Homotopic local-global parcellation of the human cerebral cortex from resting-state functional connectivity. Neuroimage 273, 120010.
Yarkoni, T., Poldrack, R.A., Nichols, T.E., Van Essen, D.C., Wager, T.D., 2011. Large-scale automated synthesis of human functional neuroimaging data. Nat. Methods 8, 665–670.
Yeo, B.T., Krienen, F.M., Sepulcre, J., Sabuncu, M.R., Lashkari, D., Hollinshead, M., Roffman, J.L., Smoller, J.W., Zöllei, L., Polimeni, J.R., 2011. The organization of the human cerebral cortex estimated by intrinsic functional connectivity. J. Neurophysiol.
Zhang, F., Moerman, F., Niu, H., Warreyn, P., Roeyers, H., 2022. Atypical brain network development of infants at elevated likelihood for autism spectrum disorder during the first year of life. Autism Res.
Zhou, Y., Yu, F., Duong, T., 2014. Multiparametric MRI characterization and prediction in autism spectrum disorder using graph theory and machine learning. PLoS One 9, e90405.